Cell Calcium 80 (2019) 71–78

Contents lists available at ScienceDirect

Cell Calcium

journal homepage: www.elsevier.com/locate/ceca

Grina/TMBIM3 modulates voltage-gated $Ca_V2.2$ Ca^{2+} channels in a G-protein-like manner

Robert Theodor Mallmann[a,1], Lucia Moravcikova[b,1], Katarina Ondacova[b], Lubica Lacinova[b], Norbert Klugbauer[a,*]

[a] Institut für Experimentelle und Klinische Pharmakologie und Toxikologie, Fakultät für Medizin, Albert-Ludwigs-Universität Freiburg, Albertstr. 25, 79104 Freiburg, Germany
[b] Center of Bioscience - Institute for Molecular Physiology and Genetics, 84005 Bratislava, Slovakia

ARTICLE INFO

Keywords:
N-type calcium channel
$Ca_V2.2$
Grina
TMBIM3
G-protein
Channel modulation

ABSTRACT

Grina/TMBIM3 is a poorly characterized transmembrane protein with a broad expression pattern in mammals and with a very ancient origin within eukaryotes. Although initially characterized as an NMDA-receptor associated subunit, there is increasing evidence that Grina/TMBIM3 is involved in the unfolded protein response and controls apoptosis via regulation of Ca^{2+} homeostasis. Here, we investigate a putative direct interaction of Grina/TMBIM3 with voltage gated Ca^{2+} channels, in particular with the $Ca_V2.2$ α1-subunit and describe its modulatory effects on the current through $Ca_V2.2$ N-type channels. Direct interaction was confirmed by co-immunoprecipitation studies and membrane localization was proven. Co-expression of Grina/TMBIM3 with $Ca_V2.2$ channels resulted in a significant decrease of the current amplitude and in a slowing of the kinetics of current activation. This effect was accompanied by a significant shift of the voltage dependencies of activation time constants towards more depolarized voltages. Application of a stimulus protocol including a strong depolarizing pulse relieved inhibition of current amplitude by Grina/TMBIM3. When Grina/TMBIM3 was present, inactivation by an action potential-like train of pulses was diminished. Both observations resemble mechanisms that are well-studied modulatory effects of G-protein βγ subunits on Ca_V2 channels. The impact of Grina/TMBIM3 and G-protein βγ subunits are rather comparable with respect to suppression of current amplitude and slowing of activation kinetics. Furthermore, both modulators had the same effect on current inactivation when evoked by an action potential-like train of pulses.

1. Introduction

Grina/TMBIM3 was described first in 1991 by Kumar and colleagues as glutamate-recognition protein and was classified as an NMDA-receptor associated subunit of a four-protein complex [1]. Grina/TMBIM3 was recognized by antibodies against the glutamate-binding protein complex, was purified by affinity chromatography using a glutamate-treated column and had a dissociation constant of 263 nM for glutamate. Hydrophobicity plots of Grina/TMBIM3 predicted a transmembrane protein with seven transmembrane segments and a large intracellular N-terminus.

In the following years however, cDNA-cloning, structural and functional work on the NMDA-receptor complex [2] changed these early views and questioned the identity of Grina/TMBIM3 as a glutamate receptor subunit. Furthermore, numerous groups investigated Grina/TMBIM3 in the past two decades, but so far, its biological function could not be conclusively clarified. For example, Grina/TMBIM3 has been described as a possible MAPK-activating protein [3], as a putative protecting protein of retinal damage in ischemia-perfusion injury [4] and as one of 28 genes preferentially expressed beneath the marginal zone in the developing cerebral cortex [5].

More recently, work focused on the presence of a conserved BAX inhibitor-1 motif in the Grina/TMBIM3 primary sequence [6,7]. The presence of this motif led to the renaming of Grina to TMBIM3 (transmembrane BAX inhibitor motif 3). The BAX motif defines Grina/TMBIM3 as part of a small family of proteins comprising at least seven mammalian members with anti-apoptotic properties. However, a more in-depth sequence and phylogenetic analysis revealed that only part of these members form a clear-cut protein family. This analysis finally resulted in the definition of a new gene family, which was named LFG,

* Corresponding author.
E-mail address: n.klugbauer@pharmakol.uni-freiburg.de (N. Klugbauer).
[1] Contributed equally.

https://doi.org/10.1016/j.ceca.2019.04.002
Received 25 January 2019; Received in revised form 1 April 2019; Accepted 7 April 2019
Available online 08 April 2019
0143-4160/

Lifeguard [6]. Hu and colleagues conclude that the high structural similarity of LFG proteins and the presence of consensus sequence motifs suggests a common function for regulation of apoptosis. The tissue expression profile of LFG proteins is rather diverse and even the subcellular localization strongly differs, indicating an evolutionary specialization of apoptotic regulation in these various compartments.

Anti-apoptotic properties were demonstrated in COS cells transfected with full-length and deletion mutants of Grina/TMBIM3 [7]. Cells were treated with hydrogen peroxide and the rate of cell death was assessed. It turned out that Grina/TMBIM3 transfected cells showed a significantly higher percentage of survival than control cells. In an *in vivo* mouse model, the Grina/TMBIM3 gene was deleted, but no obvious behavioral phenotype was detected using a modified SHIRPA test and also histological evaluation of major organ systems did not result in anomalies [7].

In contrast to the above-mentioned mouse model, manipulation of Grina/TMBIM3 in Drosophila melanogaster and Zebrafish indicated a link with ER stress and apoptosis [8]. These authors showed an upregulation of the Grina/TMBIM3 mRNA levels in cellular and animal models of ER stress. Obviously, Grina/TMBIM3 acts in concert with TMBIM6/BI-1 and both participate in the regulation of ER Ca^{2+} homeostasis and have synergistic pro-survival activity. In zebrafish, manipulation of Grina/TMBIM3 expression resulted in an increased rate of apoptosis during development and anomalies in brain morphology and neuronal survival [8].

In line with the studies of Rojas-Rivera and colleagues, Lisak and coworkers also demonstrated a crucial role of the TMBIM family for the maintenance of intracellular Ca^{2+} homeostasis in various tissues [9]. Besides a reduction of the ER Ca^{2+} content mediated by all members of the TMBIM family, with the exception of TMBIM5, all other TMBIMs also reduced the cytosolic resting Ca^{2+} concentrations. Thus, a reduction in cytosolic Ca^{2+} concentration might affect the cell´s responsiveness for apoptotic stimuli since Ca^{2+} is known to influence the manifold apoptosis pathways. Ca^{2+} influx from the extracellular space or Ca^{2+} release from the ER may initiate apoptosis by mitochondrial Ca^{2+} overload followed by cytochrome c release, loss of ATP, generation of reactive oxygen species or depolarization [10].

Due to this close link between Grina/TMBIM3 and regulation of ER and cytosolic Ca^{2+} levels, we asked for putative interaction partners of Grina/TMBIM3 that may be crucial for regulation of Ca^{2+} homeostasis. Since a major influx of Ca^{2+} ions occurs through voltage-gated Ca^{2+} channels (VGCC), we investigated a direct effect of Grina/TMBIM3 on VGCCs.

2. Materials and methods

2.1. Cell lines and cultivation

MEF cells were grown in DMEM high glucose containing 10% FCS, 1 mM sodium pyruvate and 100 U/ml penicillin–streptomycin. The CHO cell line stably transfected with human α1-Ca_V2.2-EGFP (accession number M94172), $\alpha_2\delta$-1 and β1-subunits was provided by B. Fakler, Institute of Physiology II, University of Freiburg. CHO-cells were grown in MEM ALPHA (Life Technologies) substituted with L-glutamine 200 mM, 10% FCS, 0.25 mg/ml hygromycin B, 0.7 mg/ml G418 and 0.005 mg/ml blasticidin.

For patch clamp experiments cells were harvested from culture flasks and seeded onto 13 mm acid washed and poly-L-lysine coated round glass coverslips (VWR International, Darmstadt, Germany). To transfect cells with the appropriate expression vectors, LipofectAMINE 2000 (Invitrogen) was used following manufacturer's instructions. For electrophysiological studies cells were transfected with either control pEGFP-N1 or Grina/TMBIM3-pEGFP-N1 vector. Cells were incubated for 24–48 h following transfection before electrophysiological experiments.

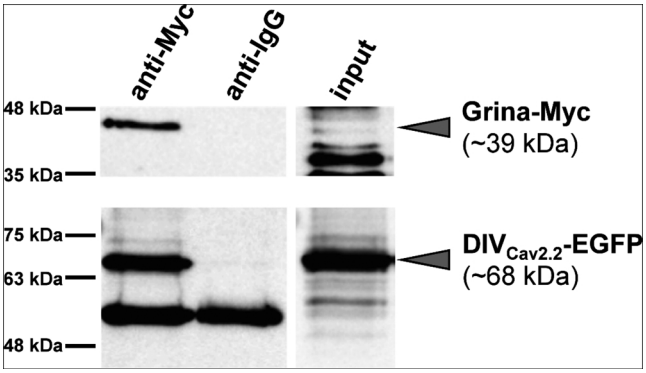

Fig. 1. Co-immunoprecipitation analysis using solubilisates of membrane-fractions obtained from CHO cells transfected with cDNA vectors encoding domain IV of Ca_V2.2 fused to EGFP (DIV$_{Cav2.2}$-EGFP) and Myc-tagged Grina/TMBIM3 (Grina-Myc). Eluates from co-immunoprecipitations with either anti-Myc (left) or IgG-control antibodies (middle) and the input controls (right) were separated on 12% SDS-polyacrylamide gels. Anti-Myc and anti-EGFP antibodies were used for detection of corresponding protein bands. The figure shows a representative example of three independent co-immunoprecipitation experiments.

2.2. Isolation and cloning of Grina/TMBIM3

Whole brain isolated from an adult male mouse (C57/ Bl6 N) was used to isolate total RNA with the RNeasy Midi kit (Qiagen) according to the manufacturer´s protocol. To perform cDNA synthesis we used the Transcriptor High Fidelity cDNA synthesis kit (Roche Diagnostics, Mannheim, Germany). A full-length Grina/TMBIM3 cDNA fragment (NP_075657.1) was generated by PCR and cloned into pEGFP-N1 (Clontech). Patch-clamp and cell-imaging experiments were performed with full-length mouse Grina/TMBIM3 fused to EGFP (pEGFP-N1, Clontech). Co-IP.experiments were performed using N-terminal myc-tagged full length Grina/TMBIM3 (pcDNA3.1, Invitrogen).

2.3. Subcellular localization of Grina/TMBIM3

To analyze the subcellular localization of Grina/TMBIM3, MEF cells were harvested from culture flasks and seeded to cell culture dishes with glass bottom (CellviewTM Cellculture dish, Greiner Bio-One, Germany). MEF cells were transfected with Grina/TMBIM3-pEGFP-N1. Transfection was performed with LipofectAMINE 2000 (Invitrogen) following manufacturer's instructions. Cells were cultured for 48 h in DMEM high glucose containing 10% FCS, 100 U/ml penicillin–streptomycin and 1 mM sodium pyruvate. The culture medium was replaced by Live Cell Imaging Solution (Thermo Fisher Scientific), following three washing steps with the same solution. To stain plasma membranes and nuclei of cells, CellMask™ Deep Red Plasma membrane Stain and NucBlue® Live reagent (Thermo Fisher Scientific) was used, following manufacturer's instructions. Stained cells were mounted in a live-cell imaging chamber with humidified atmosphere (6.5% CO_2 and 9% O_2) at 37 °C. Image acquisition was performed with a Zeiss LSM510 microscope (Carl Zeiss, Jena) equipped with a CSU-X1 Spinning Disc (Yokogawa) and a Coolsnap HQ II digital camera (Photometrics) with 640-, 488- and 405-nm laser lines. Metamorph and ImageJ software were used to process images.

2.4. Co-Immunoprecipitation (Co-IP)

CHO cells were co-transfected with vectors encoding myc-Grina/TMBIM3 and DIV$_{CaV2.2}$-EGFP (pEGFP-N1, Clontech). The Ca_V2.2-EGFP fusion protein consists of Ca_V2.2-domain-IV (accession number NP_001182128.1, amino acids 1491–1727) fused with a linker sequence (Ca_V1.2 loop I-II, accession number CAA39289.1, amino acids

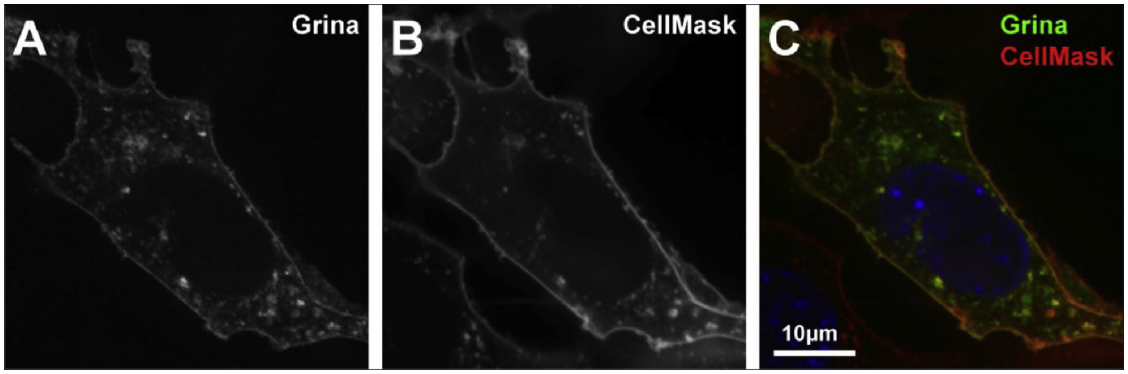

Fig. 2. Intracellular distribution of Grina/TMBIM3. MEF cells were transfected with a cDNA vector encoding EGFP-tagged Grina/TMBIM3 and were stained with CellMask Deep Red plasma membrane stain and NucBlue Live reagent 48 h after transfection. The figure shows a representative example of three independent live-cell imaging experiments. (A) Cellular distribution of Grina/TMBIM3 (Grina), (B) staining with CellMask and (C) merge of (A) and (B). Scale bar 10 µm.

405–513) to EGFP. For each co-IP-experiment, cells of two 10 cm dishes were rinsed with ice-cold PBS pH7.4 (containing proteinase inhibitor complete 1550 Roche (Roche, Mannheim, Germany)). Cells were pooled and washed two times in PBS (5 min at 500 x g at 4 °C). The thoroughly homogenized cells were centrifuged (5 min at 1000 x g at 4 °C) to obtain membrane-protein containing supernatant. Membrane-protein enriched fractions were sedimented by additional centrifugation of the supernatant (16,000 x g for 2 h at 4 °C). Such pelleted membranes were re-suspended in CL91-buffer (Logopharm, Freiburg, Germany) containing proteinase inhibitor complete 1550 and protein concentration was adjusted to approximately 1.25 mg/ml. Solubilization was carried out at 4 °C for 30 min under continuous movement, afterwards insoluble material was removed by centrifugation (110 min at 16,000 x g at 4 °C). Aliquots of solubilized protein (supernatants) and pellets were resolved in SDS-loading buffer and checked for solubilization efficiency. Equal amounts of solubilized proteins (400–600 µl) were added to 5 mg DynaBeads® Protein G (Invitrogen, Darmstadt, Germany) and 10 µg anti-myc antibody (Cell-signalling, Frankfurt, Germany) or 10 µg mouse-IgG control (Merck, Darmstadt, Germany). After immunoprecipitation, beads were washed and proteins were eluted with SDS-buffer following manufacturer's instructions.

2.5. Patch clamp experiments

HEKA EPC10 (HEKA Electronics, Lambrecht, Germany) patch clamp amplifier was used for electrophysiological experiments. Patch pipettes were made from borosilicate glass (Sutter Instruments, Novato, CA) with a resistance ranging between 1.8 and 2.2 MΩ when filled with experimental solutions. Composition of extracellular solution was (in mM): 10 HEPES, 10 $BaCl_2$, 1 $MgCl_2$, 100 TEA-Cl, and 10 D-glucose; pH 7.4 (adjusted with TEA-OH). Composition of intracellular solution was (in mM): 3 Na_2ATP, 10 HEPES, 10 EGTA, 110 CsCl, 3 $MgCl_2$, and 0.6 Tris-GTP; pH 7.3 (adjusted with CsOH). Cells with input resistance above 5 MΩ were not used for experiments. During analysis all cells with Boltzmann coefficient from Boltzmann-Ohm fit to an I–V relation lower than 3 were excluded. However, in majority of analyzed cells, this coefficient was bigger than 4. Data were recorded using Patchmaster v2 × 73.3 (HEKA Electronics, Lambrecht, Germany) and analyzed using Fitmaster v2 × 73.3 and Origin 8.1 (OriginLab Co., Northampton, MA, USA) software.

2.6. Data acquisition and analysis

A holding potential (HP) was set to −80 mV. Current-voltage (I–V) relation was measured using a series of 10 ms long depolarizing voltage pulses from a HP to voltages between −50 mV and + 80 mV. Kinetics of current activation was evaluated by fitting an ascending part of a current trace by a single exponential. Voltage dependencies of time constants evaluated at individual voltages between + 10 mV and + 60 mV were fitted by Eq. (1):

$$\tau_{act}(V) = e^{\frac{-(V-V_{act})}{dV}} + \tau^{act}(\infty) \quad (1)$$

V_{act} designates the position of each voltage dependence on a voltage axis, dV represents its steepness, and $\tau_{act}(\infty)$ corresponds to the infinitesimal value of an activation time constant to which each voltage dependence converges.

Possible G-protein-dependent channel inactivation was evaluated by a three pulse protocol depicted in Fig. 3 panel A. 50 ms long depolarizing pulse to + 20 mV (T1) was followed by 10 s long interval at a HP, a brief depolarizing prepulse to + 100 mV, and by test pulse T2 identical to T1. Extent of current facilitation by a prepulse was evaluated as a ratio of current amplitudes measured during pulses T2 and T1; i.e., I_{T2}/I_{T1}.

Cumulative voltage-dependent inactivation of $Ca_V2.2$ channels was assessed by a train of 10 action-potential-like waveforms with peak amplitudes of + 50 mV and a frequency of 100 Hz as depicted in Fig. 4.

Experimental data are presented as mean ± S.E.M. Statistical significance of the difference between two data sets was evaluated by a two-tailed unpaired Student t-test. For comparison of more than two dataset, one-way Anova followed by Tukey post test was used. Probability $p < 0.05$ was considered as significant.

3. Results

3.1. Identification and confirmation of Grina/TMBIM3 as an interactor of $Ca_V2.2$

Grina/TMBIM3 was identified as an interactor of $Ca_V2.2$ in an unbiased yeast two-hybrid screen. Bait constructs consisting of single Ca_V2 calcium channel domains were used to screen a murine brain cDNA library as described in our previous studies [11,12]. Functional expression of single Ca_V domains was verified by using Ca_V fusion proteins harbouring the ß subunit binding domain (AID). These control experiments indicated correct conformation of the Ca_V domains used and further supported our experimental strategy that single Ca_V domains mimic at least in part the configuration of the entire α1 subunit.

Our screenings indicated that domain IV of the $Ca_V2.2$ α1-subunit interacted with Grina/TMBIM3, whereas other VGCC fragments such as those from L-type $Ca_V1.2$ and P/Q-type $Ca_V2.1$ α1-subunits failed to show an interaction (data not shown). These initial results of the yeast two-hybrid system gave us a first hint for an interaction between Grina/TMBIM3 and $Ca_V2.2$. To confirm these preliminary findings, we performed co-immunoprecipitation studies using Grina/TMBIM3-Myc and $Ca_V2.2$ domain-IV-EGFP constructs co-expressed in CHO cells. Probing

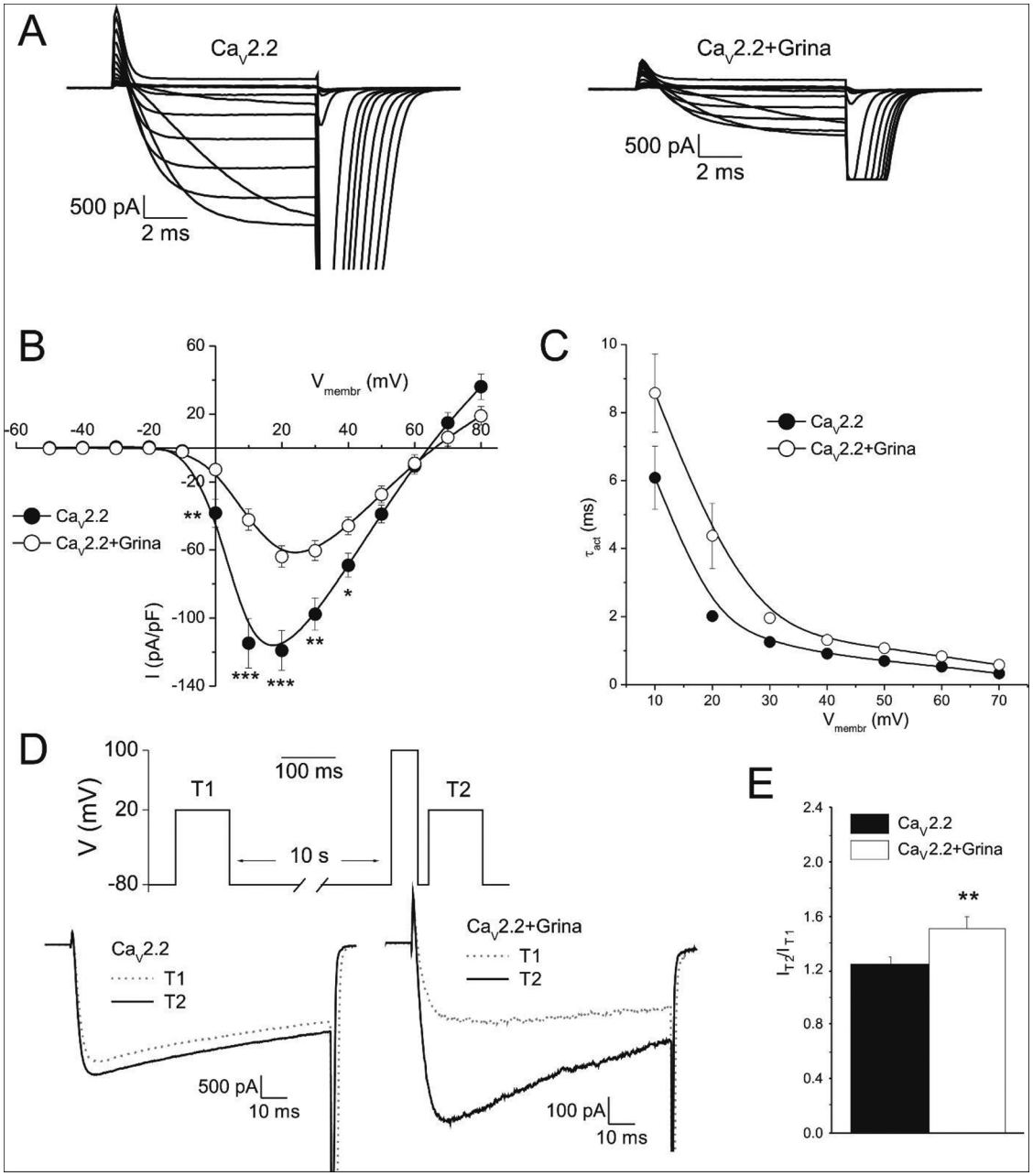

Fig. 3. (A) Representative examples of current traces recorded by an I–V protocol from CHO cells expressing the $Ca_V2.2$ channel complex transfected with pEGFP (left, control) and CHO cells expressing the $Ca_V2.2$ channel complex transfected with Grina/TMBIM3 cDNA (right).
(B) Averaged data for I–V relations measured from cells expressing $Ca_V2.2$ channel (solid circles, n = 27) and together with Grina/TMBIM3 (open circles; n = 23). Solid lines represent B-spline connectors of experimental data.
(C) Voltage dependencies of activation time constants evaluated as monoexponential fits to current traces recorded at individual depolarizing voltages from cells expressing $Ca_V2.2$ channel (solid circles) and together with Grina/TMBIM3 (open circles). Solid lines represent B-spline connectors of experimental data.
(D) Protocol used for evaluation of prepulse facilitation is depicted at the top. A 50 ms long test pulse T1 to + 20 mV was followed by 10 s long interval at HP to exclude voltage dependent inactivation during the pulse and by a conditioning 20 ms long prepulse to + 100 mV. Finally, test pulse T2 equal to T1 was applied. Below, representative examples of current traces recorded from the same cell during T1 pulse (dashed line) and T2 pulse (solid line) in the absence (left) or presence (right) of Grina/TMBIM3. Please note different time scale in panels A and D.
(E) Extent of prepulse facilitation was evaluated for each cell as ratio of current amplitudes measured during pulses T2 and T1. Black column – control, n = 22; open column – $Ca_V2.2$ channel in the presence of Grina/TMBIM3, n = 20.
* - $p < 0.05$; ** - $p < 0.01$; *** - $p < 0.001$.

solubilized membrane preparations resulted in precipitation of a Grina/TMBIM3-$Ca_V2.2$ complex (Fig. 1). Thus, co-immunoprecipitation studies confirmed our initial finding for an interaction between Grina/TMBIM3 and $Ca_V2.2$.

3.2. Grina/TMBIM3 localizes in the plasma membrane

Next, we investigated the subcellular distribution of Grina/TMBIM3 to confirm that a significant amount of protein localizes in the plasma membrane, where VGCC interaction may occur. EGFP-tagged Grina/TMBIM3 was expressed in MEF cells and green fluorescence was

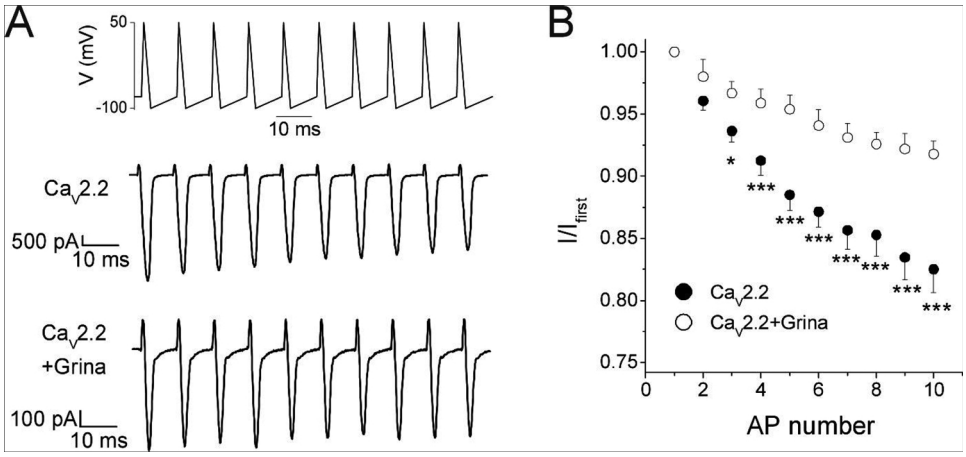

Fig. 4. (A) Voltage protocol for evaluation of current inactivation evoked by an action-potential-like-train is depicted on top. 0.5 ms long depolarization pulses from −80 mV to + 50 mV were followed by 2.5 ms long repolarization to −100 mV and by 7.5 ms long depolarization to −80 mV. This sequence was repeated 10 times. Below, representative examples of current traces activated by this protocol are shown for $Ca_V2.2$ channel (middle) and together with Grina/TMBIM3 (bottom). (B) Relative amplitudes of inward currents activated by n-th action potential were calculated as I_n/I_1 ratio. Closed circles - $Ca_V2.2$ channel (n = 26); open circles – $Ca_V2.2$ channel in the presence of Grina/TMBIM3 (n = 21) * - p < 0.05; *** - p < 0.001.

Table 1
Eq. (1) was used to calculate parameters V_{act}, dV and $\tau(\infty)$ for the groups indicated. V_{act} designates the position of each voltage dependence on a voltage axis, dV represents its steepness, and $\tau_{act}(\infty)$ corresponds to the infinitesimal value of an activation time constant to which each voltage dependence converges. Significance of differences compared to $Ca_V2.2$ (control): * - p < 0.05; ** - p < 0.01.

	V_{act} (mV)	dV (mV)	$\tau(\infty)$ (ms)
$Ca_V2.2$	23.2 ± 0.9	10.7 ± 1.1	0.61 ± 0.06
$Ca_V2.2$ + Grina	33.4 ± 2.4**	13.6 ± 1.4	0.56 ± 0.09
$Ca_V2.2$ + Gβγ	32.4 ± 2.1*	13.9 ± 1.6	0.68 ± 0.07
$Ca_V2.2$ + Gβγ + Grina	33.1 ± 4.4*	14.5 ± 2.5	0.59 ± 0.12

recorded and compared with that of CellMask (red fluorescence) (Fig. 2). As a result, Grina/TMBIM3 was visible in several intracellular compartments, but also to a significant amount in the cell membrane.

3.3. Modulatory effects of Grina/TMBIM3 on $Ca_V2.2$ channels

Finally, we focused on potential modulatory effects of Grina/TMBIM3 on $Ca_V2.2$ VGCCs. When Grina/TMBIM3 was expressed in CHO cells stably transfected with $Ca_V2.2$ channels, the amplitude of the current decreased significantly (Fig. 3A, B). We evaluated the kinetics of current activation by fitting the ascending parts of current traces measured during the I–V protocol by a monoexponential function. When Grina/TMBIM3 was coexpressed, the kinetics of current activation was slower (Fig. 3C). An apparent difference in voltage dependencies of activation time constants was mainly caused by a significant shift in voltage dependencies towards more depolarized voltages (Table 1). A shallower slope of voltage dependencies (Table 1), which points to a lowered sensitivity of the channel to membrane depolarization, may also contribute to the observed phenomenon. However, this change was not statistically significant (Table 1).

A suppressed current amplitude and slower activation kinetics are characteristic for a so-called reluctant gating state of the $Ca_V2.2$ channel. Typically, $Ca_V2.2$ channels are transferred into this state by binding of G-protein βγ subunits, which can be reversed by a strong depolarization. We tested the extent of G-protein-related channel inhibition using a voltage protocol depicted in Fig. 3D. As apparent from representative current traces (Fig. 3D) and from the averaged extent of inhibition relief by a depolarizing pre-pulse (Fig. 3E), inhibition of current amplitude by co-expression of Grina/TMBIM3 was relieved by a strong depolarization. Next, we tested the cumulative current inhibition by an action potential (AP)-like train. While repetitive depolarization inactivates voltage-dependent calcium channels, it may paradoxically facilitate current through the $Ca_V2.2$ channel by relieving G-protein-dependent inhibition [13]. When Grina/TMBIM3 was co-expressed with $Ca_V2.2$ channels, (Fig. 4A, B) inactivation caused by an AP-like train was diminished. Altogether, Grina/TMBIM3 inhibited the current amplitude by a mechanism similar to that caused by G-proteins.

Therefore, we tested the effect of co-expression of recombinant Gβγ subunits per se and together with Grina/TMBIM3. Co-expression of Gβγ subunits suppressed the current amplitude (Fig. 5A and B) and slowed the kinetics of current activation by shifting its voltage dependence (Fig. 5C and Table 1). The extent of both effects was similar to that caused by expression of Grina/TMBIM3 (Fig. 3). Both effects were not further enhanced when Gβγ subunits were expressed together with Grina/TMBIM3 (Fig. 5A–C and Table 1). As expected, co-expression of Gβγ subunits significantly enhanced G-protein-dependent current inhibition (Fig. 5D and E). When Grina/TMBIM3 protein was expressed additionally, G-protein-dependent inhibition was further enhanced only to a minor extent and this enhancement was not significant (Fig. 5D and E).

As in the case of activation, the effect of co-expression of Gβγ subunits alone or together with Grina/TMBIM3 had the same effect on inactivation evoked by an AP-like train as co-expression of Grina/TMBIM3 (Fig. 6A, B). Extent of inactivation was not significantly different between Gβγ and Gβγ + Grina/TMBIM3.

In summary, our results from the yeast split-ubiquitin system and co-localization and co-precipitation studies point to an interaction between Grina/TMBIM3 and the $Ca_V2.2$ α1-subunit. Co-expression of both proteins show modulatory effects on the current through $Ca_V2.2$ and importantly, Grina/TMBIM3 demonstrates a VGCC regulation, comparable to that of Gβγ.

4. Discussion

In our study, we provide evidence for an important modulatory function of Grina/TMBIM3 for $Ca_V2.2$ Ca^{2+} channels. Initiated by yeast two hybrid screenings we identified a $Ca_V2.2$ Ca^{2+} channel fragment that interacted with Grina/TMBIM3. These preliminary results were verified by co-precipitation studies using domain IV of $Ca_V2.2$ α1-subunit. Expression of EGFP-tagged Grina/TMBIM3 in MEF cells demonstrated its localization in intracellular compartments as well as in the cell membrane. Nielsen, Rojas-Rivera and Lisak et al. also investigated the subcellular localization but came to varying results [7–9]. The murine Grina/TMBIM3 investigated by Nielsen et al. was localized to the perinuclear region in transfected COS cells and by using organelle markers was narrowed down to the Golgi apparatus, whereas the endoplasmic reticulum could be excluded. This result was confirmed by Lisak´s studies, who transfected HA-tagged Grina/TMBIM3 in HT22 cells and found a predominant localization in the Golgi. These data partially contradict that of Rojas-Rivera, who identified myc-tagged Grina/TMBIM3 not only in the Golgi but also in the endoplasmic reticulum of transfected MEF cells. Our study now shows that Grina/

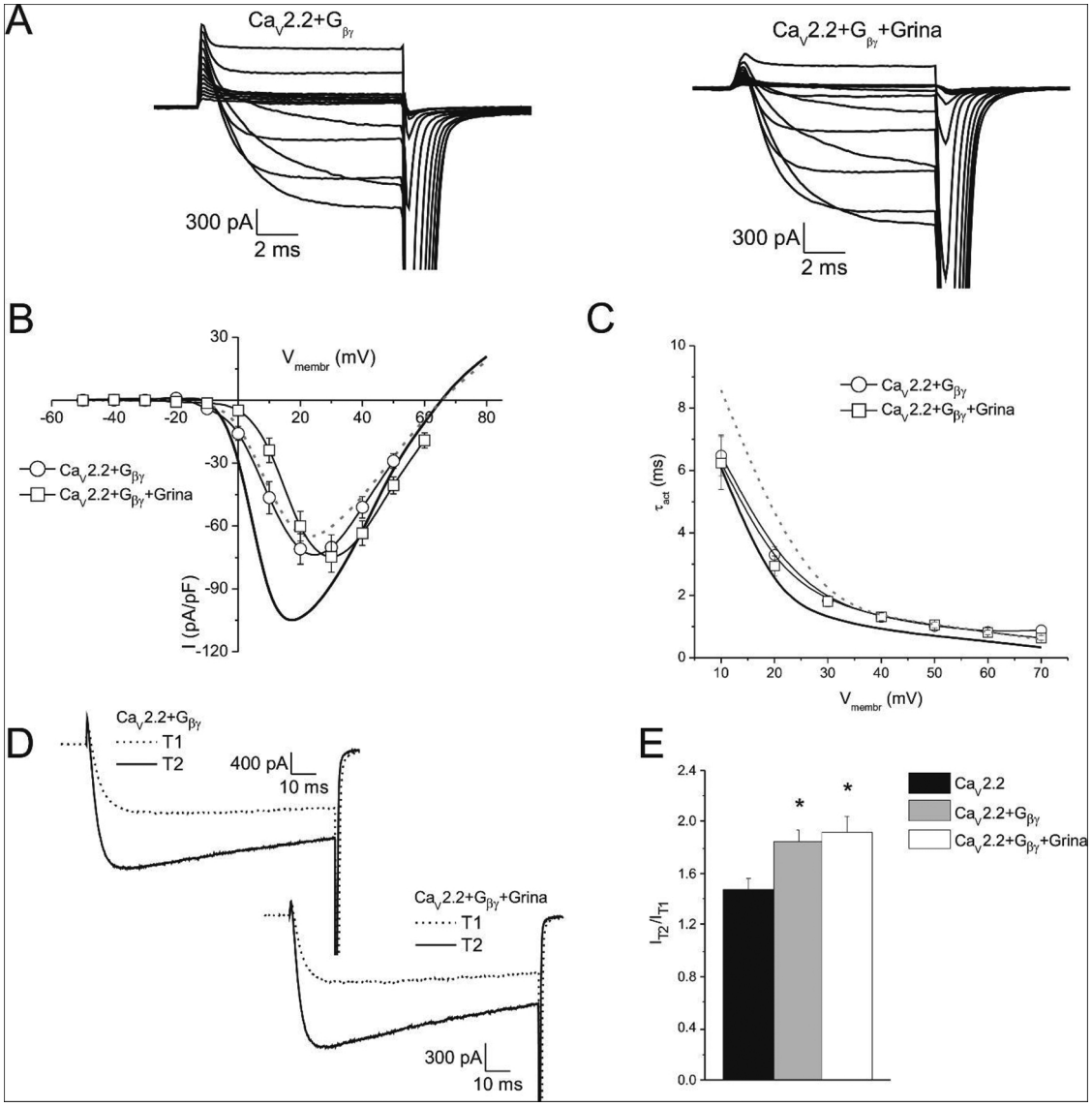

Fig. 5. (A) Examples of current traces recorded from cells expressing $Ca_V2.2$ channel in combination with Gβγ subunits (left) and Gβγ subunits together with Grina/TMBIM3 (right).

(B) Averaged data for I–V relations measured from cells expressing $Ca_V2.2$ channel with Gβγ subunits (open circles, n = 19) and Gβγ subunits together with Grina/TMBIM3 (open squares; n = 21). Solid lines represent B-spline connectors of experimental data. I–V relations from Fig. 3 are shown for comparison as a thick black line ($Ca_V2.2$ channel) and a dotted grey line ($Ca_V2.2$ channel with Grina/TMBIM3).

(C) Voltage dependencies of activation time constants evaluated as monoexponential fits to current traces recorded at individual depolarizing voltages from cells expressing $Ca_V2.2$ channel with Gβγ subunits (open circles) and with Gβγ subunits together with Grina/TMBIM3 (open squares). Solid lines represent B-spline connectors of experimental data. Voltage dependencies of activation time constants from Fig. 3 are shown for comparison as a thick black line ($Ca_V2.2$ channel) and a dotted grey line ($Ca_V2.2$ channel with Grina/TMBIM3).

(D) Examples of current traces measured with a prepulse facilitation protocol depicted in Fig. 3D. Currents measured during test pulse T1 are shown as dotted lines, currents measured during test pulse T2 are shown as solid lines. Channels and co-transfected cDNAs are marked above traces. Please note different time scale in panels A and D.

(E) Extent of prepulse facilitation was evaluated for each cell as ratio of current amplitudes measured during pulses T2 and T1. Black column – control, (n = 25); grey column – $Ca_V2.2$ channel together with Gβγ subunits, (n = 26); open column – $Ca_V2.2$ channel together with Gβγ subunits and Grina/TMBIM3, (n = 20).

* - $p < 0.05$ compared to the $Ca_V2.2$ channel.

TMBIM3 is localized also to a significant amount in the plasma membrane and not only in intracellular compartments. This result corresponds to expression profiling studies by Hu and colleagues, who identified Lfg1 (an alternative name of Grina/TMBIM3) in the plasma membrane [6].

Voltage-dependent Ca_V channels are regulated not only by voltage but also by a number of modulatory proteins [12]. Most of them are various protein kinases, which phosphorylate α1 subunits of Ca_V channels [14–16]. G-proteins represent another major group of proteins interacting with Ca_V channels [17]. Direct modulation by the Gβγ dimer dissociated from the Gα subunit is a common mechanism for regulation of neuronal Ca_V2 channels [18,19]. Most prominent modulation of current amplitude was shown for $Ca_V2.2$ channels [20,21], which, in contrast to $Ca_V2.1$ channels, exhibit a pronounced G-protein-dependent current inhibition. Activation of G-protein-coupled receptors results in dissociation of the G protein α subunit and a heterodimer consisting of β and γ (Gβγ) subunits [18]. Both of them are capable to modulate voltage-dependent calcium channels. Direct interaction of the

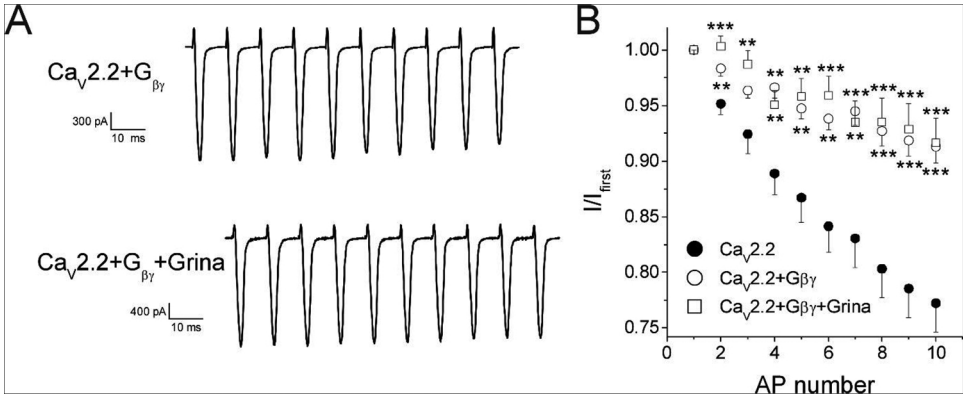

Fig. 6. (A) Representative current traces activated by action-potential-like stimulus depicted in Fig. 4A measured from cells expressing $Ca_V2.2$ channels together with Gβγ subunits or $Ca_V2.2$ channels together with Gβγ subunits and Grina/TMBIM3, as indicated. (B) Relative amplitudes of inward currents activated by n-th action potential were calculated as I_n/I_1 ratio. Solid circles - $Ca_V2.2$ channel only (n = 14); open circles – $Ca_V2.2$ channel together with Gβγ subunits (n = 14), open squares –$Ca_V2.2$ channel together with Gβγ subunits and Grina/TMBIM3 (n = 12). * - $p < 0.05$; ** - $p < 0.01$; *** - $p < 0.001$.

Gβγ dimer with a calcium channel α1 subunit mediates voltage-dependent current inhibition, which can be relieved by a high depolarization [18,20,21].

Expression of Grina/TMBIM3 in CHO cells expressing the α1 subunit of the $Ca_V2.2$ channel together with ß1 and α2δ-1 subunits suppressed current amplitude in a manner similar to that described for current inhibition by the Gβγ dimer. The amplitude inhibition was less potent at higher depolarizations, which may be explained by the occurrence of reluctant channel openings at higher depolarizations, but still corresponding to a physiological range of transmembrane potentials [22,23]. The concept of "willing" (non-Gβγ-bound) and "reluctant" (Gβγ-bound) gating states of neuronal calcium channels was introduced by Bruce Bean in 1989 [24]. Under control conditions, current exhibited fast activation kinetics corresponding to a "willing" gating state [22,25,26]. Co-expression of Grina/TMBIM3 slowed the activation kinetics of the current in a manner resembling channel transition into a "reluctant" Gβγ-bound gating state [22,25,26]. Extreme depolarization to transmembrane potentials out of the physiological range was shown to relieve G-protein-dependent current inhibition due to unbinding of the Gβγ dimer from channel´s α1 subunit [27,28]. The same phenomenon was observed in the presence of Grina/TMBIM3 in our study. A high frequency train of action potentials causes a cumulation of VGCCs in a voltage-dependent inactivated state [29]. On the other hand, such a train may also partly relieve G-protein-dependent current inhibition and cause facilitation of the calcium current [13,30,31]. In the absence of Grina/TMBIM3, a high frequency AP train inactivated the current amplitude; while in its presence, current inactivation was diminished, suggesting the occurrence of the counteracting process of current facilitation. The striking resemblance of $Ca_V2.2$ modulation by Grina/TMBIM3 and the Gβγ dimer was confirmed by their parallel expression with the $Ca_V2.2$ channel complex. Effects of both proteins on current parameters were similar and non-additive suggesting analogous underlying mechanisms.

From a structural point of view, multiple interaction sites for the Gβγ dimer with the $Ca_V2.2$ α1 subunit have been described in the literature. Those regions include the N-terminal part [32–35], the intracellular loop connecting domains I and II [36–41], the C-terminal part [20,42], and even the more intracellular part of the S1 segment in domain III [43]. The cDNA–Constructs, which were used in our initial yeast two-hybrid screening and our co-immunoprecipitation studies, included domain IV of the $Ca_V2.2$ α1 subunit; therefore, we assume that this domain at least partially forms an interaction site with Grina/TMBIM3.

5. Conclusion

In conclusion, we have shown that Grina/TMBIM3 is an interaction partner of the $Ca_V2.2$ channel α1 subunit. Strikingly, it downregulates its activity in a manner similar to that of G-protein βγ subunits. Because calcium entry through $Ca_V2.2$ channels is a major mechanism triggering transmitter release in certain synapses, Grina/TMBIM3 may contribute to regulation of synaptic transmission.

Declarations of interest

None.

Acknowledgments

We thank U. Christoph for excellent technical assistance. This work was supported by a grant from DAAD (Deutscher Akademischer Austauschdienst) to NK and LL and by two grants to LL (APVV (Slovak Research and Development Agency), APVV-15-0388 and VEGA (Scientific grant agency of the Ministry of Education, Science, Research and Sport and Slovak Academy of Sciences), 2/0143/19).

References

[1] K.N. Kumar, N. Tilakaratne, P.S. Johnson, A.E. Allen, E.K. Michaelis, Cloning of cDNA for the glutamate-binding subunit of an NMDA receptor complex, Nature 354 (1991) 70–73.
[2] M. Hollmann, S. Heinemann, Cloned glutamate receptors, Annu. Rev. Neurosci. 17 (1994) 31–108.
[3] A. Matsuda, Y. Suzuki, G. Honda, S. Muramatsu, O. Matsuzaki, Y. Nagano, T. Doi, K. Shimotohno, T. Harada, E. Nishida, H. Hayashi, S. Sugano, Large-scale identification and characterization of human genes that activate NF-kappaB and MAPK signaling pathways, Oncogene 22 (2003) 3307–3318.
[4] H. Aikawa, H. Tomita, S. Ishiguro, S. Nishikawa, E. Sugano, M. Tamai, Increased expression of glutamate binding protein mRNA in rat retina after ischemia-reperfusion injury, Tohoku J. Exp. Med. 199 (2003) 25–33.
[5] K. Tachikawa, S. Sasaki, T. Maeda, K. Nakajima, Identification of molecules preferentially expressed beneath the marginal zone in the developing cerebral cortex, Neurosci. Res. 60 (2008) 135–146.
[6] L. Hu, T.F. Smith, G. Goldberger, LFG: a candidate apoptosis regulatory gene family, Apoptosis 14 (2009) 1255–1265.
[7] J.A. Nielsen, M.A. Chambers, E. Romm, L.Y. Lee, J.A. Berndt, L.D. Hudson, Mouse transmembrane BAX inhibitor motif 3 (Tmbim3) encodes a 38 kDa transmembrane protein expressed in the central nervous system, Mol. Cell. Biochem. 357 (2011) 73–81.
[8] D. Rojas-Rivera, R. Armisen, A. Colombo, G. Martinez, A.L. Eguiguren, A. Diaz, S. Kiviluoto, D. Rodriguez, M. Patron, R. Rizzuto, G. Bultynck, M.L. Concha, J. Sierralta, A. Stutzin, C. Hetz, TMBIM3/GRINA is a novel unfolded protein response (UPR) target gene that controls apoptosis through the modulation of ER calcium homeostasis, Cell Death Differ. 19 (2012) 1013–1026.
[9] D.A. Lisak, T. Schacht, V. Enders, J. Habicht, S. Kiviluoto, J. Schneider, N. Henke, G. Bultynck, A. Methner, The transmembrane Bax inhibitor motif (TMBIM) containing protein family: tissue expression, intracellular localization and effects on the ER CA(2)(+)-filling state, Biochim. Biophys. Acta 1853 (2015) 2104–2114.
[10] M.K. Schafer, A. Pfeiffer, M. Jaeckel, A. Pouya, A.M. Dolga, A. Methner, Regulators of mitochondrial Ca(2+) homeostasis in cerebral ischemia, Cell Tissue Res. 357 (2014) 395–405.
[11] R.T. Mallmann, T. Wilmes, L. Lichvarova, A. Buhrer, B. Lohmuller, J. Castonguay, L. Lacinova, N. Klugbauer, Tetraspanin-13 modulates voltage-gated CaV2.2 Ca^{2+} channels, Sci. Rep. 3 (2013) 1777.
[12] R. Mallmann, K. Ondacova, L. Moravcikova, B. Jurkovicova-Tarabova, M. Pavlovicova, L. Lichvarova, V. Kominkova, N. Klugbauer, L. Lacinova, Four novel interaction partners demonstrate diverse modulatory effects on voltage-gated CaV2.2 Ca(2+) channels, Pflugers Arch. (2019).
[13] S. Williams, M. Serafin, M. Muhlethaler, L. Bernheim, Facilitation of N-type calcium

current is dependent on the frequency of action potential-like depolarizations in dissociated cholinergic basal forebrain neurons of the guinea pig, J. Neurosci. 17 (1997) 1625–1632.
[14] R.C. Lambert, T. Bessaih, N. Leresche, Modulation of neuronal T-type calcium channels, CNS Neurol. Disord. Drug Targets 5 (2006) 611–627.
[15] F. Hofmann, V. Flockerzi, S. Kahl, J.W. Wegener, L-type CaV1.2 calcium channels: from in vitro findings to in vivo function, Physiol. Rev. 94 (2014) 303–326.
[16] S.N. Yang, P.O. Berggren, Beta-cell CaV channel regulation in physiology and pathophysiology, Am. J. Physiol. Endocrinol. Metab. 288 (2005) E16–28.
[17] A.C. Dolphin, G.L. The, Brown Prize Lecture. Voltage-dependent calcium channels and their modulation by neurotransmitters and G proteins, Exp. Physiol. 80 (1995) 1–36.
[18] G.W. Zamponi, K.P. Currie, Regulation of Ca(V)2 calcium channels by G protein coupled receptors, Biochim. Biophys. Acta 1828 (2013) 1629–1643.
[19] J. Proft, N. Weiss, G protein regulation of neuronal calcium channels: back to the future, Mol. Pharmacol. 87 (2015) 890–906.
[20] J.F. Zhang, P.T. Ellinor, R.W. Aldrich, R.W. Tsien, Multiple structural elements in voltage-dependent Ca2+ channels support their inhibition by G proteins, Neuron 17 (1996) 991–1003.
[21] K.P. Currie, A.P. Fox, Comparison of N- and P/Q-type voltage-gated calcium channel current inhibition, J. Neurosci. 17 (1997) 4570–4579.
[22] H.M. Colecraft, P.G. Patil, D.T. Yue, Differential occurrence of reluctant openings in G-protein-inhibited N- and P/Q-type calcium channels, J. Gen. Physiol. 115 (2000) 175–192.
[23] H.M. Colecraft, D.L. Brody, D.T. Yue, G-protein inhibition of N- and P/Q-type calcium channels: distinctive elementary mechanisms and their functional impact, J. Neurosci. 21 (2001) 1137–1147.
[24] B.P. Bean, Neurotransmitter inhibition of neuronal calcium currents by changes in channel voltage dependence, Nature 340 (1989) 153–156.
[25] H.K. Lee, K.S. Elmslie, Reluctant gating of single N-type calcium channels during neurotransmitter-induced inhibition in bullfrog sympathetic neurons, J. Neurosci. 20 (2000) 3115–3128.
[26] V. Carabelli, M. Lovallo, V. Magnelli, H. Zucker, E. Carbone, Voltage-dependent modulation of single N-Type Ca2+ channel kinetics by receptor agonists in IMR32 cells, Biophys. J. 70 (1996) 2144–2154.
[27] G.W. Zamponi, T.P. Snutch, Decay of prepulse facilitation of N type calcium channels during G protein inhibition is consistent with binding of a single Gbeta subunit, Proc. Natl. Acad. Sci. U. S. A. 95 (1998) 4035–4039.
[28] A. Golard, S.A. Siegelbaum, Kinetic basis for the voltage-dependent inhibition of N-type calcium current by somatostatin and norepinephrine in chick sympathetic neurons, J. Neurosci. 13 (1993) 3884–3894.
[29] S. McDavid, K.P. Currie, G-proteins modulate cumulative inactivation of N-type (Cav2.2) calcium channels, J. Neurosci. 26 (2006) 13373–13383.
[30] D. Park, K. Dunlap, Dynamic regulation of calcium influx by G-proteins, action potential waveform, and neuronal firing frequency, J. Neurosci. 18 (1998) 6757–6766.
[31] K.P. Currie, A.P. Fox, Differential facilitation of N- and P/Q-type calcium channels during trains of action potential-like waveforms, J. Physiol. 539 (2002) 419–431.
[32] K.M. Page, F. Heblich, W. Margas, W.S. Pratt, M. Nieto-Rostro, K. Chaggar, K. Sandhu, A. Davies, A.C. Dolphin, N terminus is key to the dominant negative suppression of Ca(V)2 calcium channels: implications for episodic ataxia type 2, J. Biol. Chem. 285 (2010) 835–844.
[33] K.M. Page, C. Canti, G.J. Stephens, N.S. Berrow, A.C. Dolphin, Identification of the amino terminus of neuronal Ca2+ channel alpha1 subunits alpha1B and alpha1E as an essential determinant of G-protein modulation, J. Neurosci. 18 (1998) 4815–4824.
[34] G.J. Stephens, C. Canti, K.M. Page, A.C. Dolphin, Role of domain I of neuronal Ca2+ channel alpha1 subunits in G protein modulation, J. Physiol. 509 (Pt 1) (1998) 163–169.
[35] H.L. Agler, J. Evans, L.H. Tay, M.J. Anderson, H.M. Colecraft, D.T. Yue, G protein-gated inhibitory module of N-type (ca(v)2.2) ca2+ channels, Neuron 46 (2005) 891–904.
[36] H.W. Tedford, A.E. Kisilevsky, L.B. Vieira, D. Varela, L. Chen, G.W. Zamponi, Scanning mutagenesis of the I-II loop of the Cav2.2 calcium channel identifies residues Arginine 376 and Valine 416 as molecular determinants of voltage dependent G protein inhibition, Mol. Brain 3 (2010) 6.
[37] M. De Waard, H. Liu, D. Walker, V.E. Scott, C.A. Gurnett, K.P. Campbell, Direct binding of G-protein betagamma complex to voltage-dependent calcium channels, Nature 385 (1997) 446–450.
[38] F. Van Petegem, K.A. Clark, F.C. Chatelain, D.L. Minor Jr, Structure of a complex between a voltage-gated calcium channel beta-subunit and an alpha-subunit domain, Nature 429 (2004) 671–675.
[39] S. Herlitze, G.H. Hockerman, T. Scheuer, W.A. Catterall, Molecular determinants of inactivation and G protein modulation in the intracellular loop connecting domains I and II of the calcium channel alpha1A subunit, Proc. Natl. Acad. Sci. U. S. A. 94 (1997) 1512–1516.
[40] K.M. Page, G.J. Stephens, N.S. Berrow, A.C. Dolphin, The intracellular loop between domains I and II of the B-type calcium channel confers aspects of G-protein sensitivity to the E-type calcium channel, J. Neurosci. 17 (1997) 1330–1338.
[41] A.A. Simen, R.J. Miller, Structural features determining differential receptor regulation of neuronal Ca channels, J. Neurosci. 18 (1998) 3689–3698.
[42] N. Qin, D. Platano, R. Olcese, E. Stefani, L. Birnbaumer, Direct interaction of gbetagamma with a C-terminal gbetagamma-binding domain of the Ca2+ channel alpha1 subunit is responsible for channel inhibition by G protein-coupled receptors, Proc. Natl. Acad. Sci. U. S. A. 94 (1997) 8866–8871.
[43] S.A. Serra, N. Fernandez-Castillo, A. Macaya, B. Cormand, M.A. Valverde, J.M. Fernandez-Fernandez, The hemiplegic migraine-associated Y1245C mutation in CACNA1A results in a gain of channel function due to its effect on the voltage sensor and G-protein-mediated inhibition, Pflugers Arch. 458 (2009) 489–502.